

SCIENTIFIC REPORTS

OPEN

Unexpected 3+ valence of iron in FeO₂, a geologically important material lying “in between” oxides and peroxides

Sergey S. Streltsov^{1,2}, Alexey O. Shorikov^{1,2}, Sergey L. Skorniyakov^{1,2}, Alexander I. Poteryaev¹ & Daniel I. Khomskii³

Recent discovery of the pyrite FeO₂, which can be an important ingredient of the Earth's lower mantle and which in particular may serve as an extra source of water in the Earth's interior, opens new perspectives for geophysics and geochemistry, but this is also an extremely interesting material from physical point of view. We found that in contrast to naive expectations Fe is nearly 3+ in this material, which strongly affects its magnetic properties and makes it qualitatively different from well known sulfide analogue - FeS₂. Doping, which is most likely to occur in the Earth's mantle, makes FeO₂ much more magnetic. In addition we show that unique electronic structure places FeO₂ “in between” the usual dioxides and peroxides making this system interesting both for physics and solid state chemistry.

Recent discovery of a new iron oxide FeO₂, which does not exist at normal conditions, but can be stabilized at a very high pressure (76 GPa) and temperature (1800 K)¹ may dramatically shift our understanding of how Earth is formed and what was a source of oxygen and water in interior of our planet. FeO₂ is expected to appear in the Earth's lower mantle below 1800 km, according to¹ in the pyrite structure, and start to dominate over other Fe oxides at higher pressures. The composition of the mantle is extremely important for the seismology, since it determines convection processes. There were proposed a number of structural models based on different ratio of ferroperricite (a solid solution of FeO and MgO), bridgmanite (Mg,Fe,Al)(Al,Fe,Si)O₃, (Mg,Fe)₂SiO₄ olivine and other compounds²⁻⁵, but none of them took into account the existence of FeO₂. Moreover, physical properties of this material are completely unexplored. One might expect that they can be highly unusual, since on one hand Fe ion in FeO₂ formally should have exceptionally high oxidation state, 4+. Since the O-O distance in FeO₂ is 1.89 Å it is not likely that there can be a strong bonding between the O ions, like in molecular oxygen (where the O-O bond distance is 1.21 Å) and one may indeed expect that Fe ions will adopt 4+ valence state and then FeO₂ is in a negative charge transfer regime⁶⁻⁹. This may result in self-doping¹⁰ and also to bond or charge disproportionation^{11,12}, inversion of the crystal field splitting¹³ or nontrivial magnetic structures. On the other hand, the presence of the ligand-ligand dimers may also strongly affect physical properties of FeO₂ as it does in the actual pyrite FeS₂ (“the fool's gold”). However, O-O distance in FeO₂ is 1.89 Å, much larger than in molecular oxygen (1.21 Å) or (O₂)²⁻ ion as in the usual peroxides like BaO₂, MgO₂ (1.49 Å).

Iron peroxide was found to have the same pyrite crystal structure as FeS₂¹, see Fig. 1a, and there is not much difference between oxygen and sulfur from chemical point of view. Thus, it is tempting to consider FeO₂ as a complete analogue of FeS₂¹⁴. Since FeS₂ is known to be a diamagnetic insulator with Fe ions adopting 2+ valence state¹⁵⁻¹⁷, one might expect that the same is true for FeO₂. The first indication that such a picture is oversimplified follows from the recent theoretical study¹⁴, where FeO₂ was found to be metallic at the pressures where it does exist.

In the present paper we describe electronic and magnetic properties of FeO₂. We show that FeO₂ is completely different from FeS₂, and so are the physical properties of these compounds. The oxidation state of Fe ion in FeO₂ is not 2+, as in FeS₂, but close to 3+. This strongly affects magnetic properties of FeO₂, since having 3d⁵ electronic configuration, Fe³⁺ ions may have a magnetic moment. Our comprehensive theoretical calculations using

¹M.N. Miheev Institute of Metal Physics of Ural Branch of Russian Academy of Sciences, Ekaterinburg, Russia.

²Ural Federal University named after the first President of Russia B.N. Yeltsin, Theoretical Physics and Applied Mathematics Department, Ekaterinburg, Russia. ³II. Physikalisches Institut, Universität zu Köln, Köln, Germany. Correspondence and requests for materials should be addressed to S.S.S. (email: streltsov@imp.uran.ru)

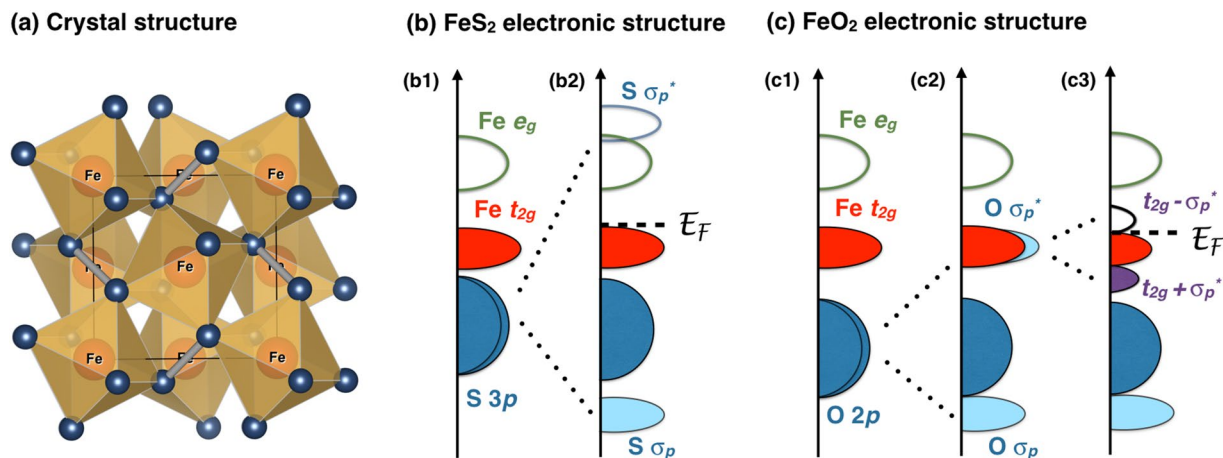


Figure 1. (a) Crystal structure of FeO₂ and FeS₂ can be visualized as a rocksalt structure like FeO with O ions replaced by S₂ (in FeS₂) or O₂ (in FeO₂) dimers. Fe ions are yellow, while O (or S) ions, forming dimers, are shown in blue. (b) and (c) Schematic band structure of FeS₂ and FeO₂.

combination of the density functional and dynamical mean-field theories (DFT + DMFT) demonstrate that there is indeed a highly nontrivial temperature dependence of the magnetic susceptibility in FeO₂. We found out that the origin of the difference in magnetic properties between FeO₂ and FeS₂ and of the metallic character of FeO₂ is a much smaller bonding-antibonding splitting for ligand σ orbitals in the peroxide dimer O₂ as compared with S₂, and a total shift of oxygen 2*p* levels relative to 3*p* levels of sulfur. This feature of the electronic structure is rather general and important for other dioxides, which can exist in Earth's mantle or in inner parts of exoplanets.

We start with FeS₂, electronic and magnetic properties of which are well understood. As discussed above, one might naively expect to have Fe⁴⁺ ions with 3*d*⁴ electronic configuration in FeS₂, since usually sulfur has a valence 2-. This would shift Fe 3*d* band very low in energy, below S 3*p*, and would result in a self-doping and a metallic conductivity⁷, which strongly disagrees with the experimental fact that FeS₂ is a semiconductor^{16,17}.

The explanation of this contradiction lies in the specific features of its crystal structure, namely the presence of the S₂ dimers. There are sulfurs 3*p* orbitals, which are directed exactly to each other in these dimers. They form such a strong bond that the antibonding σ_p^* orbitals turn out to be higher in energy than the Fe *e_g* orbitals, see Fig. 1(b2). This leads to a formal valency of sulfur "1-", (or to (S₂)²⁻ dimers), and Fe ions become 2+ with the 3*d*⁶ electronic configuration. Fe ions are in the ligand octahedra in pyrite structure. Strong crystal field splitting between the *t_{2g}* and *e_g* bands (~3.5 eV in case of FeS₂, see Supplemental materials - SM¹⁸) counteracts the Hund's rule and stabilizes the low spin configuration with all six 3*d* electrons occupying *t_{2g}* sub-shell. This makes FeS₂ diamagnetic and insulating¹⁹.

The electronic structure of FeO₂ is rather different from a sulfide counterpart. We sketched how this difference appears in Fig. 1c (while the results of the actual calculations performed within generalized gradient approximation, GGA, as well as the details of such calculations are presented in Fig. S1 in SM¹⁸), starting from the hypothetical FeO₂ having FCC lattice (like NaCl), where O ions do not form dimers and where there are basically three bands O *p*, Fe *t_{2g}*, and Fe *e_g*, see Fig. 1(c1).

First of all, as follows from our GGA calculations, the oxygen 2*p* levels are shifted down relative to the Fe 3*d* states, as compared with the 3*p* levels of sulfur. Besides, as was mentioned above, the presence of the ligand-ligand dimers in real FeO₂ results in bonding-antibonding splitting, but since oxygen 2*p* orbitals are much less extended than sulfur 3*p* orbitals, this bonding-antibonding splitting in the O₂ dimer is expected to be much smaller. As a result the antibonding O σ_p^* orbital appears not above *e_g* (like in FeS₂), but exactly in the place, where Fe *t_{2g}* bands lie, see Fig. 1(c2). Then, first of all, part of the Fe *t_{2g}* electrons would be transferred to oxygens, shifting Fe valence in the direction of 3+. Second, the hybridization between Fe 3*d* and O σ_p^* orbitals again makes bonding and antibonding combinations, which are labeled as $t_{2g} + \sigma_p^*$ and $t_{2g} - \sigma_p^*$ in Fig. 1(c3) respectively. The density of states (DOS) plot in the vicinity of the Fermi energy as obtained in conventional GGA is presented in Fig. 2(a). These $t_{2g} + \sigma_p^*$ and $t_{2g} - \sigma_p^*$ bands are centered at -2 and 1 eV in Fig. 2(a). Note that these bands have nearly the same contributions from Fe *t_{2g}* and O 2*p* (σ_p^*) states. Moreover, it is clear that peaks below and above the Fermi level are not bonding and antibonding, since there is no contribution from O 2*p* band below E_F . These are nonbonding and antibonding states.

This salient feature of FeO₂, that the antibonding σ^* orbital falls exactly into the Fe *t_{2g}* band, determines the main physical properties of FeO₂, which are very different from FeS₂, see Table 1. First of all, since there appear additional bands at the Fermi level, while the number of electrons is the same, FeO₂ is not a band insulator (as FeS₂), but a metal.

There are eight *t_{2g}* bands, each doubly degenerate with respect to spin, below the Fermi energy for the unit cell consisting of four formula units (f.u.), which are occupied by 4 electrons per each Fe ion (Fig. S1 in SM¹⁸). In addition there are four bonding $t_{2g} + \sigma_p^*$ bands with nearly 50% contribution of the Fe *t_{2g}* states (see partial DOS presented in Fig. 2), which adds approximately one more electron to each Fe ions. As a result Fe ions in FeO₂ are nearly 3+ with 3*d*⁵ electronic configuration, while in FeS₂ they are 2+.

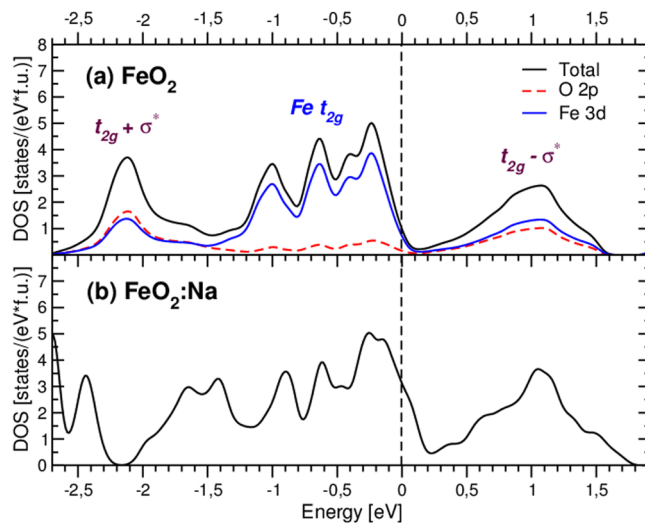


Figure 2. Total and partial density of states (DOS) in the nonmagnetic GGA calculations (a) for FeO₂ and (b) FeO₂ doped by Na (25%). Fermi energy is in zero.

	Fe valence	Electric properties	Magnetic properties
FeS ₂	2+	insulator	diamagnetic
FeO ₂	3+	metal	paramagnetic

Table 1. Comparison of different physical properties of FeS₂ and FeO₂, as follows from the DFT and DFT + DMFT calculations.

In contrast to Fe²⁺, which is nonmagnetic with t_{2g}^6 configuration at large pressure, Fe³⁺ ion even in the low-spin state has a magnetic moment. Moreover, the oxygen σ^* states are half-filled in FeO₂, and thus they can also contribute to the total magnetic moment.

Second, the Fermi level appears to be in a very specific position. On one hand it is almost in the pseudogap, so that the Stoner criterion for ferromagnetism (FM) is formally not fulfilled, and this is the reason why magnetic solutions does not survive in the GGA (we also checked stability of magnetic solutions at other q -vectors, corresponding to AFM-I and AFM-II magnetic structure of FCC lattice of Fe ions²⁰). On the other hand it is just on the border line between bands corresponding to localized t_{2g} electrons and antibonding molecular $t_{2p} - \sigma_p^*$ states. This is very important for magnetic properties of stoichiometric and non-stoichiometric FeO₂ as we will show latter.

While conventional DFT is exceptionally useful for understanding of the basics of the electronic structure in FeO₂, it does not take into account strong Coulomb correlations, which are known to be important for description of the physical properties of many transition metal compounds. We treated correlation effects using the DFT + DMFT method²¹. Hubbard U was calculated to be 6 eV, $J_H = 0.9$ eV, other details can be found in SM¹⁸.

Correlation effects manifest themselves basically via the renormalization of the GGA DOS near the Fermi level, $m^*/m \sim 1.2$ – 1.6 (depending on the orbital), resulting spectral functions are shown in Fig. S2 of SM. FeO₂ is a bad metal for experimental pressure of 76 GPa. There are 4.8 electrons in the t_{2g} shell, which certifies that Fe is 3+ in FeO₂. The local magnetic moment $\langle \sqrt{m_z^2} \rangle$ was found be $1.5 \mu_B$. The contribution from the t_{2g} orbitals to the total local magnetic moment, $\langle m_z^2 \rangle_{t_{2g}} = 1.08 \mu_B^2$, exactly corresponds to the low spin state of $3d^5$ configuration. There is, however, also an additional contribution, $\langle m_z^2 \rangle_{e_g} = 1.04 \mu_B^2$, due to a partial polarization of the ligand electrons residing e_g shell of transition metal (see detailed discussion in Supplemental materials). In spite of the fact that there are magnetic moments on Fe ions, they do not order, so that FeO₂ stays paramagnetic down to 190 K (we checked FM and AFM-I). Even lower temperatures can be reached in our calculations by using a truncated Hamiltonian, which includes only Fe t_{2g} and O $2p$ states (this choice of impurity orbitals gives the same spectral functions in vicinity of the Fermi level and very similar $\chi(T)$ as full $3d$ Hamiltonian). In this case we were able to go down to 60 K, and again FeO₂ does not order in our calculations even at these temperatures. This may seem somewhat surprising since having a rather large bandwidth (and hence hopping parameters) one might expect large superexchange interaction between Fe ions, if spins would have been localized.

In order to estimate the degree of the spin localization we calculated the analytical continuation on real frequency of the spin-spin correlator $\langle S_z(i\omega) S_z(o) \rangle = \int_0^{1/k_B T} d\tau \langle S^z(\tau) S^z(o) \rangle e^{i\omega\tau}$, where τ is an imaginary time, see right panel in Fig. 3^{22,23}. The width of this correlator is inversely proportional to the lifetime of a magnetic moment. For example in a pure metallic iron, where $t_{2g} - e_g$ crystal field splitting is small, iron ion is in a high-spin state. The magnetic moment can be considered to be localized, with the full width at half maximum (FWHM) of about 0.2 eV for the less localized γ -Fe and 0.1 eV for the more localized α -Fe^{22,24}. From the inset of

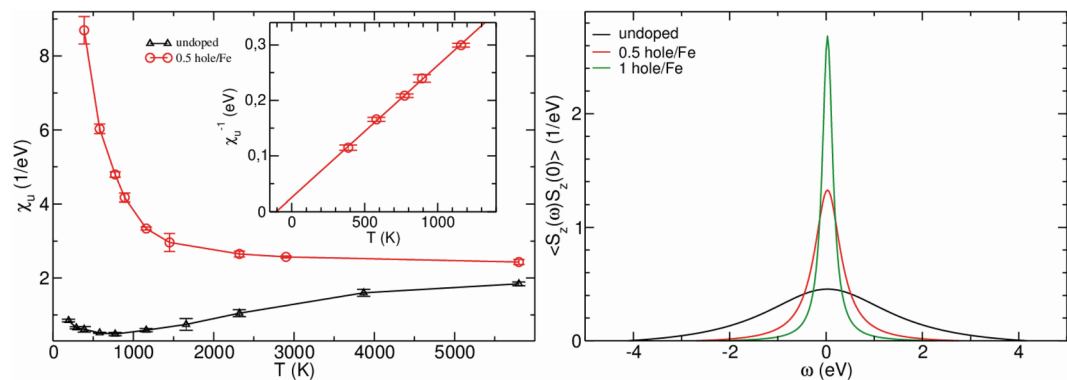


Figure 3. Results of the DFT + DMFT calculations. Left panel: uniform magnetic susceptibility for pure FeO_2 and $\frac{1}{2}$ hole/Fe doping (red circles). Inset shows magnetic susceptibility for 0.5 hole per Fe atom as a function of $1/T$. Right panel shows local magnetic susceptibility as a function of frequency for different doping.

Fig. 3 one may see that in FeO_2 FWHM of the spin-spin correlator is ~ 3 eV, which demonstrates that the magnetic moments can hardly be considered as localized.

In DMFT one can calculate the uniform magnetic susceptibility $\chi_u(T)$ as a response to an external magnetic field, which is introduced via Zeeman splitting δE in the Hamiltonian:

$$\chi_u(T) = \frac{\delta m}{\delta H} = \frac{n^\uparrow - n^\downarrow}{\delta E} \mu_B^2. \quad (1)$$

Here m is the magnetization, n^\uparrow and n^\downarrow are total occupations for spin up and down. This direct calculation of the uniform magnetic susceptibility, $\chi_u(T)$, shows that it has a nontrivial temperature dependence. Namely, with increasing temperature χ_u first decreases (for $T < T^* = 750$ K), and then starts to increase almost linearly above T^* , which resembles the behaviour of the pnictides²⁵. Detailed analysis of these data¹⁸ shows that such an unusual for 3D system behavior is due to a specific position of the Fermi level in between the localized t_{2g} and antibonding $t_{2g} - \sigma_p^*$ states. At low temperature the particle-hole excitations occur within the localized Fe t_{2g} states and $\chi_u(T)$ goes down with temperature, resembling the Curie-Weiss law. Increasing temperature further ($T > T^*$ K), we start to excite molecular-like $t_{2g} - \sigma_p^*$ states, which leads to a completely different temperature dependence.

This means that the electron and hole doping, which is likely to occur in Earth's mantle, would result in a very different temperature dependences of magnetic susceptibility, since we shift the Fermi level to the peaks corresponding to *qualitatively* different states (localized and molecular-like). There are many different elements besides Fe (5.8%) and O (44.8%) in the Earth's mantle, and one may expect that Mg ($\sim 22.8\%$), Si ($\sim 21.5\%$), Ca ($\sim 2.3\%$) or Na (0.3%)²⁶ may dope FeO_2 and change its properties dramatically. Indeed, the Fermi level in stoichiometric FeO_2 is on the steep slope of a large peak in DOS, and changing its position we strongly affect both magnetic and electronic properties.

The electron doping will shift the Fermi level to antibonding molecular-like $t_{2g} - \sigma_p^*$ states, which is unlikely to provide a large magnetic response in the simplest rigid-band shift model. Moreover, by doing this we transform Fe ion into the nonmagnetic low-spin $3d^6$ configuration, corresponding to the $2+$ oxidation state, so that only a small electron doping can increase magnetic moment. In addition the electron doping is rather unfavourable from structural point of view: the population of the strongly antibonding $t_{2g} - \sigma_p^*$ orbital would significantly weaken O_2 dimers, existing in the pyrite structure. Thus, at first sight the hole doping is expected to be much more effective for making FeO_2 magnetic: the Fermi level would then be shifted to the large peak corresponding to localized Fe t_{2g} electrons.

We checked different types of hole and electron dopings by the GGA calculations (for ferromagnetic order) performing full structural optimization, starting from the pyrite structure and substituting 25% of Fe by different ions such ions as Mg, Si, and Na. Mg doping formally changes valence of the peroxide O_2 group from 3- in FeO_2 to 2- in MgO_2 (see Fig. 4(c) and (d)), but it has no influence either on band structure or on magnetic properties of the system: unoccupied σ_p^* band corresponding to the $\text{Mg}(\text{O}_2)^{2-}$ unit appears just above the Fermi level and does not provide any holes to the Fe ions. In NaO_2 superoxide the O_2 “molecule” is 1-, see Fig. 4(b) and also ref.²⁷, and hence by Na we depopulate O π^* bond, which will be immediately refilled by the Fe t_{2g} electrons. This leads to the shift of the Fermi level downwards, see Fig. 2b, and results in the magnetic instability. In the GGA calculations the magnetic moments on Fe ions were found to be $\sim 0.4 \mu_B$. Si doping keeps FeO_2 :Si nonmagnetic, but only in unrelaxed crystal structure. After lattice optimization there appears two very different O_2 dimers, which help to form magnetic moment $\sim 0.4 \mu_B$ even in the case of the light electron doping. But the most effective are Fe vacancies (25%), which give magnetic ground state in the GGA calculations with magnetic moments $\sim 0.6 \mu_B$.

Thus, we see that there are plenty of possibilities for FeO_2 to be magnetic due to different types of doping or because of non-stoichiometry. It is hard to expect, however, that FeO_2 would order magnetically in the Earth's mantle, because of very high temperatures, ~ 1000 – 2000 K, but even in a paramagnetic state it may still provide local magnetic moments. The direct DFT + DMFT calculations within the rigid-band shift approximation (as one

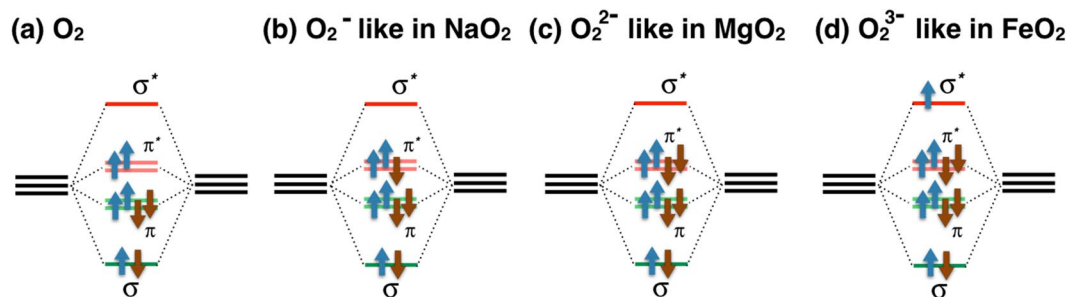


Figure 4. Occupation of oxygen 2p orbitals in different compounds with O₂ dimers. The system gains (loses) energy by occupation of green bonding (red antibonding) bonds.

can see from Fig. 2b, the band structure does not change dramatically with doping) show the drastic increase of the uniform magnetic susceptibility with hole doping, see Fig. 3. It is now Curie-Weiss like in a wide temperature range and the spin-spin correlation function demonstrates an increase of the local magnetic moments lifetime (i.e. decrease of the width of the correlator, see inset in Fig. 3) with doping.

In addition to a possible importance of our findings for geoscience, FeO₂ represents an exceptional interest also for physics and solid state chemistry, since it lies on the borderline between the stable dioxides of transition metals, such as TiO₂, VO₂, CrO₂ etc., and equally stable oxides and sulfides having pyrite structure, such as NaO₂, KO₂, FeS₂ etc. FeO₂ may thus be considered as a “bridge” between dioxides and peroxides/disulfides, and it displays properties of both.

There is a well known concept in physics, introduced by Zaanen, Sawatzky and Allen⁸, that going along a row in the periodic table from the left to the right, or increasing valence of a metal in a transition metal oxide, we go over from the Mott insulator, where the band gap is defined by Hubbard U , to a charge-transfer regime, where it is given by the charge transfer (CT) from a ligand to a metal, $\Delta_{CT} > 0$, and finally to the state, where Δ_{CT} becomes negative with ligands donating some of their electrons to a metal (so called self-doping)^{8,9}.

In peroxides the situation with the CT energy is “inverted” from the beginning: as we have seen, in FeS₂ part of electrons are transferred from sulfur to Fe. CoS₂, NiS₂, MgO₂, KO₂ and many other materials are just the same: ligand σ^* and sometimes even π^* orbitals donate (see Fig. 4) at least one electron for a metal, i.e. oxygen is 1- or even 1/2-. With FeO₂ one returns to normal transition metal oxides, where oxygen’s valency is 2-, but there is still one step to make since O is 1.5- in FeO₂. Thus, we see that FeO₂ indeed lies “in between” oxides and peroxides/disulfides, which makes it an especially interesting material from physical point of view.

A simple qualitative difference between normal (di)oxides and peroxides is the following: On one hand, when the main “structural unit” in a system is a single O ion, like in dioxides of the type of TiO₂, VO₂, its “natural” state is O²⁻, and counting from that, we see that e.g. in FeO₂ the CT energy would be negative, $\Delta_{CT} < 0$, i.e. the electrons would be transferred from O²⁻ to Fe (as it happens already in CrO₂¹⁰). But in peroxides, as well as, e.g., in FeS₂, the natural “structural unit” is the O₂ or S₂ dimer. Such dimer can be in different charge states: neutral O₂ molecule, Fig. 4a; (O₂)⁻ molecular ion (say in NaO₂, KO₂), Fig. 4b; or (O₂)²⁻ ion as in MgO₂, Fig. 4c.

The more electrons we put on such a dimer, the more we fill antibonding states, which gradually destabilizes the very O₂ dimers. But till (O₂)²⁻ it is still reasonably harmless, we fill “weakly” antibonding states (π^*), see Fig. 4. But as soon as one starts to occupy the upper σ^* states, the very dimers start to become more and more destabilised, which we indeed see in FeO₂: the O-O distance in (O₂)³⁻ dimers is 1.89 Å¹ - much larger than 1.49 Å for (O₂)²⁻ dimer in MgO₂²⁸ or 1.32 Å for (O₂)⁻ in NaO₂²⁹. Already MgO₂, having 4 electrons on antibonding π^* orbitals, see Fig. 4(c), readily decomposes at zero pressure³⁰. In FeO₂ we lose even more energy occupying antibonding σ^* orbital, see Fig. 4(d). This makes FeO₂ even less stable in the pyrite structure, than MgO₂, so that it can be stabilised only at a very high pressure.

Summarising, we see that the recently discovered pyrite-like FeO₂¹ is even more exotic than it was initially thought. Unexpected valence states, nontrivial magnetic properties, stabilization of local magnetic moments by non-stoichiometry or doping by such abundant constituents of Earth’s mantle such as Si (and Na) and finally its special place between (di)oxides and peroxides make FeO₂ extremely interesting not only for geoscience, but also for the condensed matter physics and solid state chemistry.

Data availability statement. No datasets were generated or analysed during the current study.

References

- Hu, Q. *et al.* FeO₂ and FeOOH under deep lower-mantle conditions and Earth’s oxygen–hydrogen cycles. *Nature* **534**, 241–244, <https://doi.org/10.1038/nature18018> (2016).
- Dziewonski, A. M. & Anderson, D. L. Preliminary reference Earth model. *Physics of the Earth and Planetary Interiors* **25**, 297–356, [https://doi.org/10.1016/0031-9201\(81\)90046-7](https://doi.org/10.1016/0031-9201(81)90046-7) (1981).
- Irifune, T. *et al.* Iron Partitioning and Density Changes of Pyrolite in Earth’s Lower Mantle. *Science* **327**, 193–195, <https://doi.org/10.1126/science.1181443> (2010).
- Murakami, M., Ohishi, Y., Hirao, N. & Hirose, K. A perovskitic lower mantle inferred from high-pressure, high-temperature sound velocity data. *Nature* **485**, 90–94, <https://doi.org/10.1038/nature11004> (2012).
- Wang, X., Tsuchiya, T. & Hase, A. Computational support for a pyrolitic lower mantle containing ferric iron. *Nature Geosci* **8**, 556–559, <https://doi.org/10.1038/ngeo2458> (2015).

6. Khomskii, D. Unusual valence, negative charge-transfer gaps and self-doping in transition-metal compounds. *Lithuanian Journal of Physics* **37**, 65 (1997).
7. Sawatzky, G., Green, R., Mall, E., Bc, V. & Vt, C. The Explicit Role of Anion States in High-Valence Metal Oxides. In Pavarini, E., Koch, E., van den Brink, J. & Sawatzky, G. (eds.) *Quantum Materials: Experiments and Theory Modeling and Simulation*, vol. 6, 1–36 (Verlag des Forschungszentrum, Jülich, 2016).
8. Khomskii, D. I. *Transition Metal Compounds* (Cambridge University Press, 2014).
9. Zaanen, J., Sawatzky, G. & Allen, J. Band gaps and electronic structure of transition-metal compounds. *Physical Review Letters* **55**, 418–421, <https://doi.org/10.1103/PhysRevLett.55.418> (1985).
10. Korotin, M. A., Anisimov, V. I., Khomskii, D. I. & Sawatzky, G. A. CrO₂: A Self-Doped Double Exchange Ferromagnet. *Physical Review Letters* **80**, 4305, <https://doi.org/10.1103/PhysRevLett.80.4305> (1998).
11. Bisogni, V. et al. Ground-state oxygen holes and the metal–insulator transition in the negative charge-transfer rare-earth nickelates. *Nature Communications* **7**, 13017, <https://doi.org/10.1038/ncomms13017> (2016).
12. Kawakami, T. et al. Two-Step Suppression of Charge Disproportionation. *J. Phys. Soc. Jpn.* **85**, 034716, <https://doi.org/10.7566/JPSJ.85.034716> (2016).
13. Ushakov, A. V., Streltsov, S. V. & Khomskii, D. I. Crystal field splitting in correlated systems with negative charge-transfer gap. *J. Phys.: Condens. Matter* **23**, 445601, <https://doi.org/10.1088/0953-8984/23/44/445601> (2011).
14. Jang, B. G., Kim, D. Y. & Shim, J. H. Metal-insulator transition and the role of electron correlation in FeO₂. *Phys. Rev. B* **95**, 075144, <https://doi.org/10.1103/PhysRevB.95.075144> (2017).
15. Burgardt, P. & Seehra, M. S. Magnetic susceptibility of iron pyrite (FeS₂) between 4.2 and 620 K. *Solid State Communications* **22**, 153 (1977).
16. Bullett, D. W., Khan, M. A., Schlegel, A. & Wachter, P. Optical properties, phonons and electronic structure of iron pyrite (FeS₂). *J. Phys. C: Solid State Phys.* **9**, 3363 (1976).
17. Ferrer, I. J., Nevskaja, D. M., las Heras, C. & Sanchez, C. About the band gap nature of FeS₂ as determined from optical and photoelectrochemical measurements. *Solid State Communications* **74**, 913–916 (1990).
18. see Supplemental materials.
19. Eyert, V., Höck, K.-H., Fiechter, S. & Tributsch, H. Electronic structure of FeS₂: The crucial role of electron-lattice interaction. *Physical Review B* **57**, 6350–6359, <https://doi.org/10.1103/PhysRevB.57.6350> (1998).
20. Smart, J. S. *Effective Field Theories of Magnetism*. Studies in physics and chemistry, 216 (Saunders, 1966).
21. Anisimov, V. I., Poteryaev, A. I., Korotin, M. A., Anokhin, A. O. & Kotliar, G. First-principles calculations of the electronic structure and spectra of strongly correlated systems: dynamical mean-field theory. *Journal of Physics: Condensed Matter* **9**, 7359 (1997). <http://iopscience.iop.org/0953-8984/9/35/010>
22. Katanin, A. A. et al. Orbital-selective formation of local moments in alpha-iron: First-principles route to an effective model. *Physical Review B - Condensed Matter and Materials Physics* **81**, 045117, <https://doi.org/10.1103/PhysRevB.81.045117> (2010).
23. Georges, A., Krauth, W. & Rozenberg, M. J. Dynamical mean-field theory of strongly correlated fermion systems and the limit of infinite dimensions. *Reviews of Modern Physics* **68**, 13–125, <https://doi.org/10.1103/RevModPhys.68.13> (1996).
24. Igoshev, P. A., Efremov, A. V., Poteryaev, A. I., Katanin, A. A. & Anisimov, V. I. Magnetic fluctuations and effective magnetic moments in γ -iron due to electronic structure peculiarities. *Phys. Rev. B* **88**, 155120, <https://doi.org/10.1103/PhysRevB.88.155120> (2013).
25. Skornyakov, S. L., Katanin, A. A. & Anisimov, V. I. Linear-Temperature Dependence of Static Magnetic Susceptibility in LaFeAsO from Dynamical Mean-Field Theory. *Phys. Rev. Lett.* **106**, 47007, <https://doi.org/10.1103/PhysRevLett.106.047007> (2011).
26. Jackson, I. *The Earth's Mantle: Composition, Structure, and Evolution* (Cambridge University Press, 2000). <https://books.google.ru/books?id=RlixwPYF2AC>.
27. Solov'yev, I. V., Pchelkina, Z. V. & Mazurenko, V. V. Magnetism of sodium superoxide. *CrysEngComm* **16**, 522, <https://doi.org/10.1039/b000000x> (2014).
28. Vannerberg, N.-G. The Formation and Structure of Magnesium Peroxide. *Park. Kern.* **14**, 99 (1959).
29. Ziegler, M., Rosenfeld, M., Känzig, W. & P. F. Strukturuntersuchungen an Alkalihyperoxiden. *Helv. Phys. Acta* **57**, 49 (1976).
30. Wriedt, H. A. The Mg-O (Magnesium-Oxygen) system. *Bull. Alloy Phase Diagr.* **8**, 227 (1987).

Acknowledgements

We thank V. Irkhin and I. Mazin for various stimulating discussions. The study of electronic and magnetic properties of FeO₂ performed by S.V.S. was supported by the grant of the Russian Science Foundation (project no. 17-12-01207), while work of D.I.Kh. was supported by the Deutsch Forschungsgemeinschaft through the CRC 1238 program.

Author Contributions

S.V.S. conceived the model describing electronic structures of FeO₂ and FeS₂. S.V.S. and D.I.Kh. discussed and analysed implications of features of the electronic structure for physical properties of FeO₂. The DFT calculations were performed by S.V.S. and A.O.Sh. The DFT + DMFT calculations were carried out by A.O.Sh., A.I.P., A.O.Sh., S.V.S., and S.L.S. analysed magnetic properties of FeO₂. S.V.S. and D.I.Kh. wrote the manuscript with help of all co-authors.

Additional Information

Supplementary information accompanies this paper at <https://doi.org/10.1038/s41598-017-13312-4>.

Competing Interests: The authors declare that they have no competing interests.

Publisher's note: Springer Nature remains neutral with regard to jurisdictional claims in published maps and institutional affiliations.



Open Access This article is licensed under a Creative Commons Attribution 4.0 International License, which permits use, sharing, adaptation, distribution and reproduction in any medium or format, as long as you give appropriate credit to the original author(s) and the source, provide a link to the Creative Commons license, and indicate if changes were made. The images or other third party material in this article are included in the article's Creative Commons license, unless indicated otherwise in a credit line to the material. If material is not included in the article's Creative Commons license and your intended use is not permitted by statutory regulation or exceeds the permitted use, you will need to obtain permission directly from the copyright holder. To view a copy of this license, visit <http://creativecommons.org/licenses/by/4.0/>.

© The Author(s) 2017